

Cobalt cyanoaurate: Crystal structure of a component from cobalthardened gold electroplating baths

S. C. Abrahams, L. E. Zyontz, and J. L. Bernstein

Citation: *The Journal of Chemical Physics* **76**, 5458 (1982); doi: 10.1063/1.442894

View online: <http://dx.doi.org/10.1063/1.442894>

View Table of Contents: <http://scitation.aip.org/content/aip/journal/jcp/76/11?ver=pdfcov>

Published by the **AIP Publishing**

Articles you may be interested in

[High resolution in situ magneto-optic Kerr effect and scanning tunneling microscopy setup with all optical components in UHV](#)

Rev. Sci. Instrum. **80**, 023902 (2009); 10.1063/1.3077148

[Controlled large-scale synthesis and magnetic properties of single-crystal cobalt nanorods](#)

J. Appl. Phys. **98**, 074311 (2005); 10.1063/1.2073968

[Structural characterization of periodic arrays of magnetic dots](#)

J. Appl. Phys. **87**, 4216 (2000); 10.1063/1.373055

[Electrodeposition of nanoscale magnetic structures](#)

Appl. Phys. Lett. **73**, 3279 (1998); 10.1063/1.122744

[Piezoelectric \$\text{KCo}\[\text{Au}\(\text{CN}\)_2\]_3\$: Room temperature crystal structure of a cobalthardened gold electrodeposition process component](#)

J. Chem. Phys. **73**, 4585 (1980); 10.1063/1.440697



Cobalt cyanoaurate: Crystal structure of a component from cobalt-hardened gold electroplating baths

S. C. Abrahams, L. E. Zyontz,^{a)} and J. L. Bernstein^{b)}

Bell Laboratories, Murray Hill, New Jersey 07974

(Received 16 December 1981; accepted 4 February 1982)

Cobalt cyanoaurate (I) $\text{Co}[\text{Au}(\text{CN})_2]_2$ is a new material derived from cobalt-hardened gold electroplating bath solutions that crystallizes in the hexagonal system with space group $P6_322$ and six formula weights in a unit cell with $a = 8.434 \pm 0.004$ and $c = 20.695 \pm 0.006$ Å at 298 K. The integrated intensities of a full sphere of reciprocal space, within a radius of $(\sin \theta)/\lambda = 0.85$ Å⁻¹, were measured using graphite monochromated $\text{MoK}\alpha$ with a CAD-4 diffractometer. The resulting total of 12 037 structure factors gave 1969 terms after averaging, of which 717 were accepted as reliably observed. Patterson and Fourier series were used to solve the crystal structure, which was refined by the method of least squares: the final agreement factor $R = 0.0358$. The atomic thermal vibrations are highly anisotropic. The $\text{Au}(\text{CN})_2^-$ ion departs slightly but significantly from linearity with a C–Au–C angle of $173.1 \pm 1.5^\circ$ and mean Au–C–N angle of $170.6 \pm 1.7^\circ$. The cyano groups also form tetrahedral $\text{Co}(\text{NC})_4^{2-}$ ions: conversion to the octahedral $\text{Co}(\text{NC})_6^{2-}$ ion occurs at high concentrations of K^+ in solution. The crystal radius of high-spin Co(II) decreases by 0.15 Å as the coordination changes from octahedral to tetrahedral, for a two-coordinated N radius of 1.245 Å. The mean Au–C distance is 2.003 ± 0.016 Å with C–N = 1.124 ± 0.021 Å and Co–N = 1.973 ± 0.013 Å. The mismatch between Au–Au separations in $\text{Co}[\text{Au}(\text{CN})_2]_2$ and in (111) of elementary Au is less than 8%. The identical but rotated sequence of Au–Au separations at the $c/3$ and $2c/3$ levels in $\text{Co}[\text{Au}(\text{CN})_2]_2$ coincides within 2.4% with the corresponding spacings in the element normal to (111) at the $a\sqrt{3}$ and $2a\sqrt{3}$ levels. These small mismatches could result in epitaxial overgrowth leading to gold hardening and incorporation of the observed impurities in the electrodeposit.

INTRODUCTION

Electrodeposited gold is widely used in the electronics industry as the surface-finish material in separable connectors and dry-reed sealed contacts because of its chemical resistance to all types of ambient conditions.^{1,2} The addition of cobalt ions to plating baths of $\text{KAu}(\text{CN})_2$ can increase the hardness to about four times that of annealed bulk gold, with a corresponding increase in resistivity: the resulting hard gold contains about 0.6 at. % cobalt.^{1,3} The mechanisms by which electrodeposited gold undergo hardening remain in doubt despite numerous studies, although both grain size and the presence of codeposited impurities appear to have major roles. Hard gold typically has a grain size less than 1 μm and contains codeposited cobalt, carbon, and nitrogen. Soft gold deposits are typified by larger columnar crystals of the pure element.

Hard gold baths of acidic cyanoaurate(I) ions, in combination with cobalt ions, operate close to the solubility limits of $\text{KCo}[\text{Au}(\text{CN})_2]_3$ and other cyanoaurate complexes.⁴ Eisenmann has shown that $\text{KCo}[\text{Au}(\text{CN})_2]_3$, obtained by precipitation, results in the formation of $\text{Co}[\text{Au}(\text{CN})_2]_2$ on recrystallization from water.⁴ Determination of the atomic arrangement in these two cyanoaurates is of considerable interest, in view of their possible involvement in the deposition of hard gold. The crystal structure of $\text{KCo}[\text{Au}(\text{CN})_2]_3$ has been published.⁵ The present paper reports the results of a determination of the structure of $\text{Co}[\text{Au}(\text{CN})_2]_2$.

EXPERIMENTAL

Deep violet (No. 208)⁶ hexagonal prisms of $\text{Co}[\text{Au}(\text{CN})_2]_2$ with dimensions generally close to $0.1 \times 0.1 \times 0.3$ mm, were grown by Eisenmann from $\text{KCo}[\text{Au}(\text{CN})_2]_3$ dissolved in water at 363 K.⁴ Slightly larger pseudo-hexagonal platelets containing the c axis in the plane of the plate, with the a axis inclined to the plate, also grow from solution. The hexagonal axis in the platelets is normal to a crystal edge. A sphere of diameter⁷ 0.184(6) mm was ground and mounted with random orientation on a Pyrex capillary. All integrated intensities in a full sphere of reciprocal space bounded by $(\sin \theta)/\lambda = 0.85$ Å⁻¹ were measured using an Enraf–Nonius CAD-4 diffractometer controlled by a PDP 11/40-8e minicomputer operating under Enraf–Nonius software.⁸ Initial efforts to include all reflections with $(\sin \theta)/\lambda \leq 1.00$ Å⁻¹ were abandoned since those outside the final radius were excessively weak. $\text{MoK}\alpha$ radiation reflected from a graphite monochromator was used with an ω - 2θ scan having an angular range of $1.10^\circ + 0.35^\circ \tan \theta$. The maximum time spent on a reflection was 480 s, giving a counting-statistics precision of 2% or better. The algorithm used for measuring the integrated intensities has been given elsewhere.⁹ Four standard reflections were measured hourly: the strongest varied, on average, less than 1.4% and the weakest 3.7% over the entire experiment. No corrections were made for these variations, but corrections were made for Lorentz, polarization and absorption effects. The transmission factors ranged from 0.021 to 0.065.

A total of 12 037 structure factors were measured, resulting in 1969 independent values after averaging. Standard deviations were derived from the expression:

^{a)}Present address: Colgate–Palmolive Company, 909 River Road, Piscataway, N.J. 08824.

^{b)}Present address: Western Electric Company, 475 South Street, Morristown, N.J. 07960.

$\sigma^2 F_{\text{meas}}^2 = V_1 + V_2(F_{\text{meas}})^4 + \text{larger of } [V_3(F_{\text{meas}})^4 \text{ or } V_4]$, where V_1 is the variance given by the counting statistics, $V_2 = 38 \times 10^{-4}$, $V_3 = 319 \times 10^{-4}$, and V_4 is the variance derived from differences among equivalent members in each form.¹⁰ A total of 717 independent reflections had $F_{\text{meas}}^2 > 2\sigma F_{\text{meas}}^2$. The remainder were omitted, as unobserved and hence unreliable, from further analysis. The magnitudes of the symmetry independent but Bijvoet-pair related F_{meas} and σF_{meas} are given in Ref. 11, on the final least-squares derived absolute scale.

CRYSTAL DATA

Co[Au(CN)₂]₂ has formula weight (fw) = 556.937. The hexagonal unit cell has lattice constants $a = 8.434(4)$ and $c = 20.695(6)$ Å at 298 K. The spacings of 25 reflections with $20^\circ < 2\theta < 42^\circ$ were measured with MoK α radiation using the CAD-4 diffractometer for the value of a : a modified version¹² of the Bond precision lattice constant diffractometer¹³ gave the value of c [as compared with 20.720(10) Å based on the CAD-4 results]. The volume of the unit cell is 1274.86 Å³. $D_m = 4.32(9)$, $D_x = 4.352$ g cm⁻³, for six fw per unit cell. The absorption coefficient¹⁴ for MoK α radiation is 36.03 mm⁻¹ and, for the sphere used, $\mu R = 3.315$. $F(000) = 1422e$.

The Laue symmetry of Co[Au(CN)₂]₂ was found to be 6/mmm, and the only systematic absences are 00. l with $l = 3n$. A choice could be made among the likely space groups $P6_2$, $P6_4$, $P6_222$, and $P6_422$, on the basis of the vector distribution in the Patterson function, as that of $P6_422$.

SOLUTION AND REFINEMENT OF THE Co[Au(CN)₂]₂ STRUCTURE

Recognition of the major interatomic vectors in the three-dimensional Patterson function as Au–Au interactions, followed by least-squares refinement, gave a value for the agreement factor¹⁰ $R = 0.199$. The difference Fourier series clearly revealed the Co atom position: least-squares refinement, with isotropic temperature factors for both heavy atoms, reduced R to 0.108 and the corresponding difference Fourier series allowed the two independent nitrogen atoms and corresponding carbon atoms to be located. Calculations were made using Enraf–Nonius software¹⁵ on the PDP 11/40 minicomputer.

TABLE I. Structural refinement indicators for Co[Au(CN)₂]₂ at 298 K.^a

| Parameters varied ^b | Number of parameters | R^c | wR | S |
|-------------------------------------|----------------------|--------|--------|-------|
| xyz, B | 23 | 0.0655 | 0.1033 | 0.964 |
| $\bar{x}\bar{y}\bar{z}, B$ | 23 | 0.0886 | 0.1334 | 1.244 |
| xyz, β_{ij} | 53 | 0.0358 | 0.0516 | 0.491 |
| $\bar{x}\bar{y}\bar{z}, \beta_{ij}$ | 53 | 0.0626 | 0.0893 | 0.850 |

^aSee Ref. 10 for definitions of R , wR , and S .

^bA single scale factor is varied for each model. No correction for extinction was necessary.

^cFor the 717 independent F_{meas} given in Ref. 11.

TABLE II. Atomic coordinates for Co[Au(CN)₂]₂ at 298 K.^a

| Atom | x | y | z |
|------|--------------|--------------|-------------|
| Au | 0.316 33(10) | 0.000 58(12) | 0.125 93(4) |
| Co | 0.500 0 | 0 | 0.374 1(2) |
| N(1) | 0.140 0(26) | 0.708 1(28) | 0.017 2(9) |
| N(2) | 0.448 4(30) | 0.289 5(30) | 0.236 1(10) |
| C(1) | 0.218 0(23) | 0.820 4(26) | 0.053 2(10) |
| C(2) | 0.393 7(57) | 0.190 2(57) | 0.195 1(11) |

^aValues without errors are determined by symmetry and may not be varied.

Least-squares refinement of the position coordinates and isotropic thermal parameters for all six atoms was completed on the Honeywell 6000 computer using ORFLS-3,¹⁶ to eliminate the possibility of reaching a false minimum with the least-squares program of Ref. 15.¹⁷ Atomic scattering factors used in the final refinements were those for neutral atoms as given in the *International Tables for X-Ray Crystallography*.¹⁴ Agreement factors for the four models investigated are listed in Table I. In each case, the magnitude of the largest shift in any parameter was less than 1% of the corresponding error. Application of an isotropic extinction correction resulted in a g value within 1.2 σ of zero. Inspection of the larger magnitudes in Ref. 11 confirms that the effects of extinction in the crystal studied are indeed negligible. A δR normal probability plot,¹⁸ displaying the agreement between all pairs of F_{meas} and F_{calc} , was generally quite linear except for a few terms. The two with poorest agreement were $F(922)$ and $F(41\bar{1})$, with $F_{\text{meas}} - F_{\text{calc}}$ magnitudes of 4.1 and 2.1 σF_{meas} , respectively: all other differences were less than $2\sigma F_{\text{meas}}$. The distribution of error in the measurements and in the model are hence normal. The slope of the δR plot is 0.461, indicating that σF_{meas} has been overestimated on average by a factor of 2.2: a possible source of this overestimation is the magnitude derived for V_3 in the estimate of variance (see Experimental).

The final magnitudes of the atomic position coordinates are given in Table II and the anisotropic temperature coefficients in Table III.

ABSOLUTE SENSE OF ATOMIC ARRANGEMENT

The anomalous scattering contribution of MoK α radiation by the Co, Au, C, and N atoms to the measured structure factors causes $F(hkl) \neq F(\bar{h}\bar{k}\bar{l})$: hence, an atomic arrangement with coordinates $x_i y_i z_i$ will give a different fit to the magnitudes in Ref. 11 than one with coordinates $\bar{x}_i \bar{y}_i \bar{z}_i$. It is convenient to use Hamilton's method¹⁹ to test the hypothesis that the latter model fits the observations better than the former by comparing the experimental value of $wR(\bar{x}\bar{y}\bar{z})/wR(xyz)$ to that calculated at the half-percent significance level for 717 independent F_{meas} and 53 variables, i.e., $R_{1.694\ 0.005} = 1.0061$. Table I give 1.731 for the experiment, hence the hypothesis can be rejected with confidence. The hypothesis is similarly rejected for the isotropic thermal vibration models, on the basis of Table I, since $R_{\text{exp}} = 1.291$ and $R_{1.694\ 0.005} = 1.0059$. The atomic coordinates in Table III hence represent the absolute

Table III. Anisotropic temperature coefficients in $\text{Co}[\text{Au}(\text{CN})_2]_2$ at 298 K.^a

| Atom | β_{11} | β_{22} | β_{33} | β_{12} | β_{13} | β_{23} |
|-------------------|--------------|--------------|--------------|--------------|--------------|--------------|
| Au | 1353(15) | 977(10) | 117(2) | 493(12) | -33(4) | -69(3) |
| Co | 998(66) | 1017(42) | 91(9) | 578(60) | 0 | 0 |
| N(1) | 88(28) | 131(32) | 19(6) | 15(24) | -15(10) | -4(9) |
| N(2) | 161(38) | 149(35) | 19(6) | 113(34) | 7(12) | 17(11) |
| C(1) ^b | 52(24) | 66(28) | 14(5) | -29(19) | -22(8) | -8(9) |
| C(2) | 309(86) | 313(84) | 13(6) | 238(66) | 39(23) | 49(22) |

^aBased on the exponential expression $-\langle \beta_{11} h^2 + \beta_{22} k^2 + \beta_{33} l^2 + 2\beta_{12} hk + 2\beta_{13} hl + 2\beta_{23} kl \rangle$. The coefficients are $\times 10^5$ for Au and Co, and $\times 10^4$ for N and C. See also footnote to Table II.

^bThe coefficients for C(1) are slightly nonpositive definite. A reduction in the magnitude of β_{13} by one e.s.d. restores the overall temperature factor of this atom to physical reality.

arrangement of atoms in $\text{Co}[\text{Au}(\text{CN})_2]_2$ at 298 K for the Miller indices and F_{meas} listed in Ref. 11, as illustrated in Fig. 1.

AMPLITUDES OF VIBRATION

Hamilton's¹⁹ method may also be used to test the hypothesis that the atomic vibrations in $\text{Co}[\text{Au}(\text{CN})_2]_2$ at 298 K are isotropic rather than anisotropic, based on the agreement indicators of Table I. The experimental ratio $wR(\text{isotropic})/wR(\text{anisotropic}) = 2.002$ greatly exceeds the value of $R_{30\ 664\ 0.005} = 1.040$, hence the hypothesis can be rejected confidently at the half-percent significance level. The RMS amplitudes of thermal vibration and corresponding standard errors, derived from the values in Table III and the variance-covariance matrix of the final cycle of least squares refinement by means of the ORFFE program,²⁰ are given in Table IV. The ratio of maximum to minimum amplitude for each atom varies from about 1.2 for Co to 5.2 for C(1), confirming that these atomic vibrations are anisotropic. The absolute magnitudes are comparable to, or slightly greater than, those found in $\text{KCo}[\text{Au}(\text{CN})_2]_3$.⁵ In the latter crystal, the rms radial thermal displacements are 0.163 Å for Au, 0.133 Å for Co,

0.173 Å for N, and 0.165 Å for C as compared with 0.175 Å for Au, 0.155 Å for Co, 0.194–0.195 Å for N, and 0.167–0.236 Å for C in $\text{Co}[\text{Au}(\text{CN})_2]_2$. It may be seen in Fig. 2(a) that the principal axes of thermal vibration for N(1) and N(2) are approximately normal to the Co–N bonds.

LINEARITY OF CYANOAUATE ION

The ionic dimensions of the $\text{Au}(\text{CN})_2^-$ ion in a number of compounds have recently been shown⁵ to correspond to a nearly linear atomic array with weighted mean Au–C distance of 1.989(9) Å and weighted mean C–N distance of 1.156(12) Å. These interatomic distances do not differ significantly from those in $\text{Co}[\text{Au}(\text{CN})_2]_2$, as given in Table V. The C–Au–C and N–C–Au angles, in previously investigated compounds, have not departed significantly from 180°⁵; the Au atoms in $\text{KAu}(\text{CN})_2$ ²¹ and in $\text{K}[\text{Au}(\text{CN})_2\text{Cl}_2] \cdot \text{H}_2\text{O}$ ²² are located at inversion centers and hence the C–Au–C angle in these crystals is required to be linear. The electronic structure of the assumed-linear $\text{Au}(\text{CN})_2^-$ ion has recently been studied.²³ It was concluded that inner *p* orbitals participate in the valence molecular orbitals of σ_u symmetry and that $\text{Au}(5d-6s)$ hybridization of the last occupied molecular orbital of σ_g^* symmetry is of importance.

The departure of C(1)–Au–C(2) from 180° (see Table V) amounts to 4.6 estimated standard deviations (e.s.d.'s) and must be regarded as significant unless the e.s.d. has been underestimated. The weighted mean Au–C–N angle of 170.6(1.7)° departs by 5.5 e.s.d.'s from linearity. The magnitude of *S* in Table I

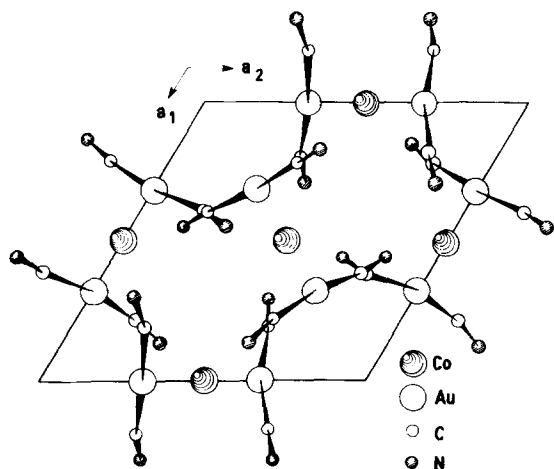


FIG. 1. View of the contents of a unit cell of $\text{Co}[\text{Au}(\text{CN})_2]_2$, with part of adjacent cells, projected along the hexagonal direction through $c/2$. The representation used for the four kinds of atoms is given by the key.

TABLE IV. Root-mean-square amplitudes of thermal vibration along the principal ellipsoid axes in $\text{Co}[\text{Au}(\text{CN})_2]_2$ at 298 K.

| Atom | 1 | 2 | 3 |
|-------------------|------------|------------|------------|
| Au | 0.144(1) Å | 0.177(1) Å | 0.200(2) Å |
| Co | 0.141(7) | 0.153(13) | 0.169(4) |
| N(1) | 0.130(29) | 0.206(29) | 0.236(35) |
| N(2) | 0.138(75) | 0.193(33) | 0.238(20) |
| C(1) ^a | 0.042(65) | 0.182(28) | 0.220(33) |
| C(2) | 0.098(90) | 0.202(117) | 0.342(25) |

^arms amplitudes for C(1) correspond to a value of $\beta_{13} = -0.0014$ (see Table III).

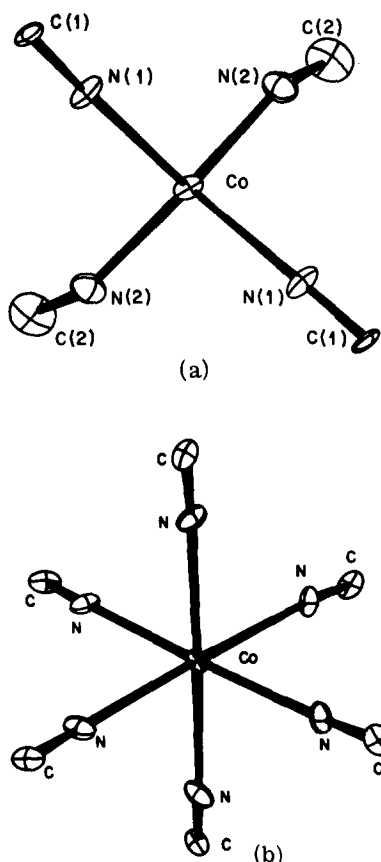


FIG. 2. (a) Tetrahedral $\text{Co}(\text{NC})_4^{2-}$ ion, as in $\text{Co}[\text{Au}(\text{CN})_2]_2$. (b) Octahedral $\text{Co}(\text{NC})_6^{4-}$ ion, as in $\text{KCo}[\text{Au}(\text{CN})_2]_3$.

shows that σ_{meas} is probably too small, on average, by about a factor of 2. One or more replications of the atomic coordinates in Table II, under noncorrelated conditions, are necessary to estimate the error in the resulting mean coordinates more accurately. If the error in these e. s. d.'s is assumed small, it must be concluded that both the C-Au-C and Au-C-N angles are significantly deformable from linearity provided the interaction between the cyano group and adjacent Co atom is strong enough, see the next section.

TETRAHEDRAL-OCTAHEDRAL COORDINATION OF COBALT

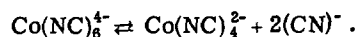
The ratio of tetrahedrally/octahedrally coordinated cobalt(II) in aqueous solution has recently been studied²⁴ as a function of temperature and ionic concentration of accompanying SO_4^{2-} or Cl^- ions. For a given concentration of either anion, the ratio was found to decrease more or less linearly with increasing inverse temperature. In the case of $\text{KCo}[\text{Au}(\text{CN})_2]_3$, the Co^{2+} is octahedrally coordinated by the nitrogen of six cyano groups with Co-N distances of 2.124(10) Å⁵; the N-Co-N angles are 86.5(5)° and 178.5(1.3)° [cf. Fig. 2(b)]. By contrast, in $\text{Co}[\text{Au}(\text{CN})_2]_2$ the Co^{2+} is tetrahedrally coordinated by the nitrogen of four cyano groups, with pairs of Co-N distances at 1.963(18) and 1.986(20) Å, respectively [Fig. 2(a)]. It may be noted that $\text{KCo}[\text{Au}(\text{CN})_2]_3$ crystals are grown by re-

TABLE V. Interatomic distances less than 3.2 Å and corresponding angles in $\text{Co}[\text{Au}(\text{CN})_2]_2$ at 298 K.

| | | | |
|--------------|----------------|--------------|-----------------|
| Au-C(2) | 1.999(32) Å | Co-N(1) | 1.963(18) Å × 2 |
| -C(1) | 2.004(19) | -N(2) | 1.986(20) × 2 |
| Au-Au | 3.109(3) | N(1)-C(1) | 1.125(25) |
| -Au | 3.165(2) | N(2)-C(2) | 1.120 (39) |
| C(1)-Au-C(2) | 173.1(1.5)° | C(1)-N(1)-Co | 176.1(1.9)° |
| N(1)-Co-N(1) | 104.5(1.1) | C(2)-N(2)-Co | 160.4(2.7) |
| -N(2) | 109.5(1.1) × 2 | N(1)-C(1)-Au | 170.1(1.9) |
| -N(2) | 112.7(1.0) × 2 | N(2)-C(2)-Au | 172.7(3.7) |
| N(2)-Co-N(2) | 107.9(1.2) | | |

crystallizing the precipitate obtained from concentrated solutions of $\text{KAu}(\text{CN})_2$ and $\text{Co}(\text{CN})_2$ with a two-molar KCl aqueous solution at 373 K.⁵ Crystals of $\text{Co}[\text{Au}(\text{CN})_2]_2$ are grown from a solution of $\text{KCo}[\text{Au}(\text{CN})_2]_3$ in water at 363 K.⁴ The primary controlling factor in the formation of $\text{Co}[\text{Au}(\text{CN})_2]_2$ from $\text{KCo}[\text{Au}(\text{CN})_2]_3$, with resulting transition from octahedrally to tetrahedrally coordinated cobalt(II), is hence the concentration of K^+ ions in the solution.

Measurement of the absorption spectrum of aqueous solutions of $\text{KCo}[\text{Au}(\text{CN})_2]_3$ as a function of K^+ concentration is expected to provide further data on the equilibrium:



In the case of the cobalt(II)-chloride octahedral/tetrahedral equilibrium, ΔH has been reported²⁴ in the range 46–62 kJ mol⁻¹.

The Co(II) radius decreases sharply in the coordination change from octahedral to tetrahedral. The Co(II)-N octahedral distance of 2.124(10) Å in $\text{KCo}[\text{Au}(\text{CN})_2]_3$ decreases to the weighted mean value of 1.973 Å in $\text{Co}[\text{Au}(\text{CN})_2]_2$, a reduction of 0.15 Å. Shannon's crystal radii¹⁵ of 0.885 Å for high-spin octahedral Co(II) and 0.72 Å for high-spin tetrahedral Co(II) thus correspond to an average crystal radius of 1.245 Å for the two-coordinated cyanide-nitrogen

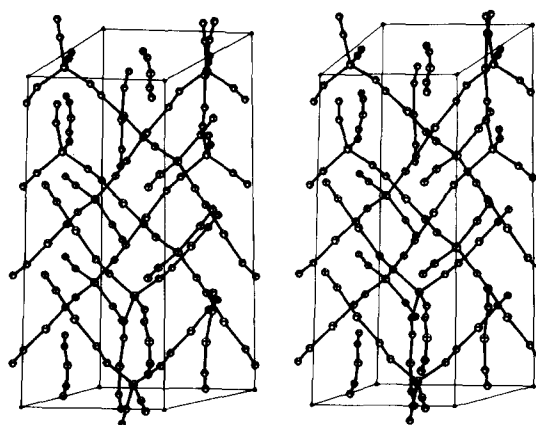


FIG. 3. Stereoscopic view of the atomic arrangement in $\text{Co}[\text{Au}(\text{CN})_2]_2$, with outline of unit cell.

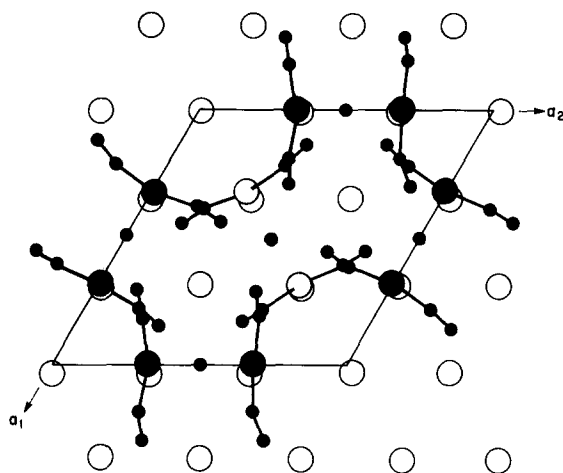


FIG. 4. Superposition of $\text{Co}[\text{Au}(\text{CN})_2]_2$ structure on (111) of elementary gold. Open circles denote Au in the element, heavily shaded circles represent Au at $z=0$ in $\text{Co}[\text{Au}(\text{CN})_2]_2$, medium shaded circles are at $z=c/3$, lightly shaded circles are at $z=2c/3$, and small filled circles represent Co, C, and N (see also Fig. 1).

atom. The tetrahedral Co(II) coordination results in a linkage of $\text{Au}(\text{CN})_2^-$ ions into infinite, interconnected, atomic chains as illustrated in Fig. 3.

PIEZOELECTRIC COEFFICIENT IN $\text{Co}[\text{Au}(\text{CN})_2]_2$

A single independent piezoelectric coefficient $d_{14} = -d_{25}$ is allowed in space group $P6_422$. Attempts to detect this coefficient, either by use of a locally modified Giebe-Sheibe apparatus²⁶ or by direct electrometer measurement on the small and fragile single crystals available, were unsuccessful.

POSSIBLE ROLE OF $\text{Co}[\text{Au}(\text{CN})_2]_2$ IN GOLD ELECTRODEPOSITION

The incorporation of Co, C, and N in electrodeposited gold and the hardening due to reduced grain size, if originating in the presence of $\text{Co}[\text{Au}(\text{CN})_2]_2$ in the hardening bath, is readily visualized as taking place through the process of epitaxial overgrowth. Consideration of the interatomic Au-Au spacings in crystalline $\text{Co}[\text{Au}(\text{CN})_2]_2$ and in elementary gold reveals striking similarities. The closest Au-Au distance in the element is 2.884 Å, forming an hexagonal array in the (111) plane. In $\text{Co}[\text{Au}(\text{CN})_2]_2$, the Au-Au separations along (10.0) are 3.109 Å across the twofold (located at the Co atoms) and 5.341 Å across the 6₄-fold (located at the origin) axes (cf. Fig. 1). The displacements of Au in $\text{Co}[\text{Au}(\text{CN})_2]_2$ from the positions occupied in the element are hence 7.8% and 7.4% respectively for these two separations: further, the a axis repeat (of 8.434 Å) in $\text{Co}[\text{Au}(\text{CN})_2]_2$ is within 2.6% of matching a linear triplet of minimum Au-Au spacings in the element (see Fig. 4).

An identical sequence of Au-Au spacings occurs in layers at $c/3$ (i.e., 6.898 Å) and $2c/3$ above the base [i.e., (00.1)] plane in $\text{Co}[\text{Au}(\text{CN})_2]_2$ (see Fig. 4). The $c/3$ spacing (6.898 Å) is within 2.4% of the corresponding spacing ($a\sqrt{3}=7.0639$ Å) in the element. The rela-

tively small mismatch in Au-Au separation and direction between those in $\text{Co}[\text{Au}(\text{CN})_2]_2$ and in the element could hence result in epitaxial overgrowth of the $\text{Co}[\text{Au}(\text{CN})_2]_2$ crystals on the dominant growing gold (111) surfaces. Such overgrowth would cause premature termination of the electrodeposited gold single crystal growth and hence an increase in hardness due to the resulting smaller crystallite size. Overgrowth would also lead to the incorporation of Co, C, and N in the electrodeposit.

ACKNOWLEDGMENT

It is a pleasure to thank E. T. Eisenmann for preparing the crystals of $\text{Co}[\text{Au}(\text{CN})_2]_2$.

- ¹R. Duva and D. G. Foulke, *Plating* **55**, 1056 (1968).
- ²M. Antler, in *Gold Plating*, edited by F. H. Reid and W. Goldie (Electrochemistry, Ayr, Scotland, 1974), pp. 259-294.
- ³C. C. Lo, J. A. Augis, and M. R. Pinnel, *J. Appl. Phys.* **50**, 6887 (1979).
- ⁴E. T. Eisenmann, *J. Electrochem. Soc.* **124**, 1957 (1977).
- ⁵S. C. Abrahams, J. L. Bernstein, R. Liminga, and E. T. Eisenmann, *J. Chem. Phys.* **73**, 4585 (1980).
- ⁶K. L. Kelly and D. B. Judd, *Natl. Bur. Stand. Circ.* **553**, (1965) (including supplement, Standard Sample No. 2106).
- ⁷Error values here and elsewhere in this paper, given in parentheses, correspond to the least significant digits in the function value.
- ⁸*Enraf-Nonius CAD-4 Operators Manual* (Enraf-Nonius, Delft, 1980).
- ⁹R. Liminga, S. C. Abrahams, and J. L. Bernstein, *J. Chem. Phys.* **67**, 1015 (1977).
- ¹⁰S. C. Abrahams, J. L. Bernstein, and E. T. Keve, *J. Appl. Crystallogr.* **4**, 284 (1971).
- ¹¹See AIP Document No. PAPS JCPSA-76-5458-4 for 4 pages of measured and calculated structure factors of $\text{Co}[\text{Au}(\text{CN})_2]_2$ at 298 K. Order by PAPS number and journal reference from American Institute of Physics, Physics Auxiliary Publication Service, 335 East 45th Street, New York, N.Y. 10017. The price is \$1.50 for microfiche or \$5.00 for a photocopy. Airmail is additional. Make checks payable to the American Institute of Physics.
- ¹²R. L. Barns, *Mater. Res. Bull.* **2**, 273 (1967).
- ¹³W. L. Bond, *Acta Crystallogr.* **13**, 814 (1960).
- ¹⁴*International Tables for X-Ray Crystallography*, edited by J. A. Ibers and W. C. Hamilton (Kynoch, Birmingham, 1974), Vol. IV.
- ¹⁵*Enraf-Nonius Structure Determination Package*, edited by B. Frenz (Molecular Structure Corporation, College Station, Texas, 1980).
- ¹⁶W. R. Busing, K. O. Martin, and H. A. Levy, *J. Appl. Crystallogr.* **6**, 309 (1973).
- ¹⁷C. Svensson, S. C. Abraham, and J. L. Bernstein, *J. Solid State Chem.* **36**, 195 (1981).
- ¹⁸S. C. Abrahams and E. T. Keve, *Acta Crystallogr. Sect. A* **27**, 157 (1971).
- ¹⁹W. C. Hamilton, *Acta Crystallogr.* **18**, 502 (1965).
- ²⁰W. R. Busing, C. K. Johnson, W. E. Thiessen, and H. A. Levy, *J. Appl. Crystallogr.* **6**, 309 (1973).
- ²¹A. Rosenzweig and D. T. Cromer, *Acta Crystallogr.* **12**, 709 (1959).
- ²²C. Bertinotti and A. Bertinotti, *C. R. Acad. Sci. Paris B* **273**, 33 (1971).
- ²³D. Guenzburger and D. E. Ellis, *Phys. Rev. B* **22**, 4203 (1980).
- ²⁴T. W. Swaddle and L. Fabes, *Can. J. Chem.* **58**, 1418 (1980).
- ²⁵R. D. Shannon, *Acta Crystallogr. Sect. A* **32**, 751 (1976).
- ²⁶E. Giebe and A. Scheibe, *Z. Phys.* **33**, 760 (1925).